

Dhanjoo N. Ghista (Ed.)

Biomedical and Life Physics

**Proceedings of the Second Gauss Symposium,
2–8th August 1993, Munich**

Reprint



On Inferring the Kinetic Scheme of an Ion Channel from Postsynaptic Currents

M. Bier, G. Borst, K. Kits

Many drugs (e. g. valium) do their work by affecting the kinetics of the neurotransmitter gated ion channels involved in synaptic transmission. Much of the knowledge that we have about the kinetics of these channels has been obtained by patch clamp experiments on excised patches of membrane [1]. In these experiments one can control the concentration of neurotransmitter and follow the behavior of individual ion channels with a good signal to noise ratio. Mathematical methods are available [2] and continue to be developed [3] to relate open and closed times to the kinetic scheme of the involved ion channel. However, excised patches most likely contain extrasynaptic receptors (which may have different properties from synaptic ones) and a constant concentration of neurotransmitter applied to an excised patch is a very artificial situation.

We recorded postsynaptic currents (PSCs) in the whole cell configuration (Fig. 1), where instead of an excised patch we have complete cell "hanging" on our pipet [4]. The seal between the membrane and the pipet is often more stable in this setup than it is with patch recordings. In the whole cell configuration the clamped cell can be kept within the surrounding tissue and, like in the *in vivo* situation, every time a neighboring cell releases neurotransmitter a postsynaptic current (PSC) occurs (see Fig. 2). In our experiments the clamped cells were melanotropes from the intermediate lobe of the pituitary gland of *Xenopus laevis* and the observed currents derived from GABA mediated chloride channels. These neuroendocrine cells are very small ($\sim 5 \mu\text{m}$) and we therefore had very low noise levels, so low in fact that the last 5 channels in the tail of the PSC could be seen to open and close individually (see Fig. 2). As the GABA dissociates from the receptor and

diffuses out of the synaptic cleft we see the PSCs "die out". Below we only consider this so-called decay phase of the PSC. We assume that a neurotransmitter molecule doesn't rebind after it has dissociated. So the decay is a result only of the kinetics of the neurotransmitter-receptor complex. Next we show a mathematical method to "derive" a kinetic scheme from average and variance of a collection of PSCs.

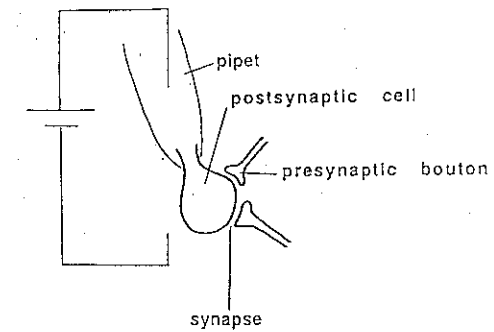


Figure 1 The setup for the experiment, every time neurotransmitter is released at a presynaptic bouton a postsynaptic current is measured.

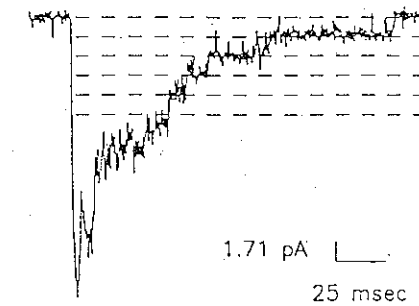


Figure 2 A typical postsynaptic current. Because of the low noise level we can see the actual discreteness of the process for the last five closing channels.

Processes on a molecular level have an innate stochasticity and this is why PSCs that start at the same amplitude decay differently. The average of a large sample of PSCs that all start at the same amplitude always appears to be well fitted with the same double exponential:

$$\bar{X}(t) = A_1 e^{-\lambda_1 t} + A_2 e^{-\lambda_2 t}, \quad (1)$$

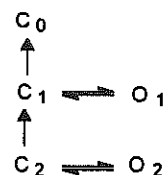
where as a convention we take $\lambda_1 > \lambda_2$ and $t=0$ is taken to be at the amplitude of the PSC. The quantities λ_1, λ_2 and $C = A_1 / (A_1 + A_2)$ turn out to always be the same, no matter what the initial amplitude of the PSC is. The amplitude can be varied with a remaining degree of freedom $A_1 + A_2$. In terms of a kinetic scheme (i. e. a Markov process in continuous time with one absorbing state) the double exponential decay is logically equivalent with the following scheme:



where going into the absorbing state corresponds to the dissociation of the neurotransmitter. Given this scheme there are two possibilities:

- 1.) HIGH EFFICACY, both X_2 and X_3 are states where the channel is open.
- 2.) LOW EFFICACY, in one of the neurotransmitter bound states the channel is closed.

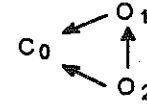
Many of the schemes that researchers have studied are special cases of either of these two models. Sequential models like $C \leftarrow O \rightleftharpoons C$ and $C \leftarrow C \rightleftharpoons O$ are special cases of the low efficacy model where one of the transition rates in (2) equals zero. The following scheme has been studied extensively [5] and seems consistent with a lot of experimental results on GABA mediated chloride channels.



The subscript indicates the number of bound GABA molecules. This scheme seems sensible; opening is a separate step that takes place after binding. In computer simulations to mimic real PSCs the times spent in C_1 and C_2 during the decay phase are almost

negligible and the extra exponents λ that these states bring about are so large (i. e. a very fast decay) that they can never be resolved in an experiment.

So in the decay phase the behavior of this scheme effectively boils down to:



i. e. a special case of the high efficacy model.

We cannot discriminate between the high and low efficacy model on the basis of just the averages of samples of PSCs. We have to go to the second moment, the variance, to make the distinction. To set ourselves up mathematically we have to first relate the observed constants λ_1, λ_2 and $C = A_1/(A_1 + A_2)$ to the transition rates of the kinetic scheme.

For the kinetic scheme of Eq. 2 the time evolution of the averages in states 2 and 3 is determined by

$$\begin{pmatrix} \dot{x}_2 \\ \dot{x}_3 \end{pmatrix} = \begin{pmatrix} -(k_{21} + k_{23}) & k_{32} \\ k_{23} & -(k_{32} + k_{31}) \end{pmatrix} \begin{pmatrix} x_2 \\ x_3 \end{pmatrix}.$$

With the initial conditions $X_2(0) = N$ and $X_3(0) = M$ we obtain for the solution of Eq. 3

$$\begin{aligned} x_2(t) &= \frac{1}{\lambda_1 - \lambda_2} \left[\left\{ N(\lambda_1 - k_{32} - k_{31}) - Mk_{32} \right\} e^{-\lambda_1 t} \right. \\ &\quad \left. + \left\{ -N(\lambda_2 - k_{32} - k_{31}) + Mk_{32} \right\} e^{-\lambda_2 t} \right] \\ x_3(t) &= \frac{1}{\lambda_1 - \lambda_2} \left[\left\{ M(\lambda_1 - k_{21} - k_{23}) - Nk_{23} \right\} e^{-\lambda_1 t} \right. \\ &\quad \left. + \left\{ -M(\lambda_2 - k_{21} - k_{23}) + Nk_{23} \right\} e^{-\lambda_2 t} \right] \end{aligned} \quad (3)$$

where λ_1 and λ_2 are the eigenvalues of the matrix.

They have the form

$$\lambda_{1,2} = \left\{ (k_{21} + k_{23} + k_{32} + k_{31}) \pm \sqrt{\left((k_{21} + k_{23} + k_{32} + k_{31})^2 - 4(k_{21}k_{32} + k_{21}k_{31} + k_{23}k_{31}) \right)} \right\} / 2$$

with

$$\lambda_1 + \lambda_2 = k_{21} + k_{23} + k_{32} + k_{31}$$

$$\lambda_1 \lambda_2 = k_{21}k_{32} + k_{21}k_{31} + k_{23}k_{31}$$

As a convention we take $\lambda_1 > \lambda_2$.

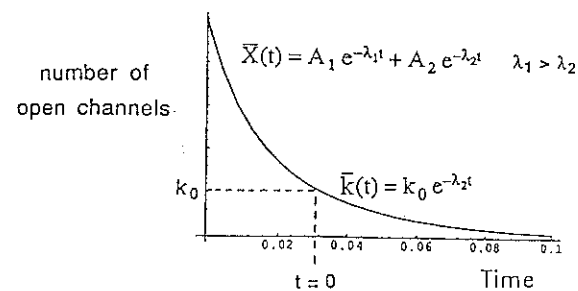


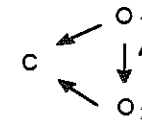
Figure 3 The idea behind our "tailvariance" analysis. Postsynaptic currents are intercepted at a fixed level of k_0 open channels, where a new $t = 0$ is set up. Each of the involved postsynaptic currents has a large enough amplitude that the fast λ_1 component is negligible when $X = k_0$. From $t = 0$ onward the variance is measured.

The quantity $C = A_1 / (A_1 + A_2)$ is related to the ratio $\rho = X_2(0) / X_3(0)$, i. e. to the distribution of bound channels over the two neurotransmitter bound states at the amplitude of the PSC. This is a consequence of risephase dynamics that we don't know anything about. To rid ourselves of this unknown we shift our analysis to the tail of the PSC (see Fig. 3), i. e. to the part of the PSC where the faster decaying $A_1 \exp(-\lambda_1 t)$ component has become negligible. At the same rate as at which the $A_1 \exp(-\lambda_1 t)$ becomes negligible the ratio $X_2(t) / X_3(t)$ (i. e. the ratio of the number of channels in state 2 and the number of channels in state 3) converges to a constant ρ' .

This constant ρ' depends only on the transition rates k_{ij} . In the tail the value of ρ' is "forgotten" and both $X_2(t)$ and $X_3(t)$ decay exponentially (so variance = average) with an exponent λ_2 .

Our procedure will be to take a large number of PSCs that start at a sufficiently large amplitude. All of these PSCs are intercepted in their tail at the same altitude m_0 where for all of the involved PSCs the fast component is negligible (see Fig. 3). This interception point will be the new $t = 0$. We then look at how the variance among these PSCs evolves in time. For both the high and low efficacy model we expect a variance that first increases from $\sigma^2(0) = 0$ as the PSCs diverge from one another due to their stochasticity, but then again goes to zero as at $t \rightarrow \infty$ the PSCs all die out. Next we will explain how for the low efficacy model the variance reaches a significantly higher maximum.

For the high efficacy model



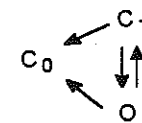
the tailvariance is easily evaluated analytically. Suppose we are in the tail of the PSC and only one channel is open at $t = 0$. Then the probability that that channel is still open at time t is $p(t) = \exp(-\lambda_2 t)$. The variance is the average of the squares minus the square of the average, hence

$$\sigma_1^2(t) = 1^2 \cdot p(t) - (1 \cdot p(t))^2 = \exp(-\lambda_2 t) - \exp(-2\lambda_2 t).$$

Variances add up, so with m_0 channels at $t = 0$ instead of 1, we obtain:

$$\sigma_{k_0}^2(t) = m_0 (\exp(-\lambda_2 t) - \exp(-2\lambda_2 t)).$$

For the low efficacy model



all of the m_0 open channels are in the one state O at time $t = 0$. A number averaging $\rho' k_0$ of neurotransmitter bound channels is still in C_1 at $t = 0$ and these channels can still flow in and out of O after $t = 0$. We thus expect a higher variance for the low efficacy model. Below we show how this variance can be derived quantitatively.

We define $P_{33}(t)$ as the probability that a channel that is in X_3 at $t = 0$ is also in X_3 at time t and $P_{23}(t)$ as the probability that a channel that is in X_2 at $t = 0$ is in X_3 at time t . $P_{33}(t)$ can be easily evaluated by substituting $N = 0$ and $M = 1$ in the equation for $X_3(t)$ under Eq. 3

$$P_{33}(t) = \frac{1}{\lambda_1 - \lambda_2} \cdot \{(\lambda_1 - k_{21} - k_{23})e^{\lambda_1 t} - (\lambda_2 - k_{21} - k_{23})e^{\lambda_2 t}\}.$$

Similarly, by substituting $N = 1$ and $M = 0$ in the equation $X_3(t)$ under Eq. 4 we find

$$P_{23}(t) = \frac{-k_{23}}{\lambda_1 - \lambda_2} (e^{-\lambda_1 t} - e^{-\lambda_2 t}).$$

The variance among the channels in the open state that were in X_3 at $t = 0$ is

$$\sigma_{33}^2(t) = MP_{33}(t)\{1 - P_{33}(t)\}.$$

The variance among the channels in the open state that were in X_2 at $t = 0$ is

$$\sigma_{23}^2(t) = NP_{23}(t)\{1 - P_{23}(t)\}.$$

Adding these two, we obtain the variance in the number of open channels for any M and N

$$\sigma_m^2(t) = \bar{m}(t) - MP_{33}^2(t) - NP_{23}^2(t).$$

The IPSCs will be intercepted in the tail, at a fixed amplitude. At this point only the slow component is important. From then on, the average number of open channels is $\bar{m}(t) = m_0 \exp(-\lambda_2 t)$ and the variance in the tail will be

$$\sigma_m^2(t) = m_0 e^{-\lambda_2 t} - m_0 P_{33}^2(t) - n_0 P_{23}^2(t).$$

Although the number of open channels at the point of interception (m_0) will be the same for all IPSCs of an experiment, the number of closed channels at that point (n_0) may vary. Because the decay of both the number of closed and the number of open channels is exponential in the tail of IPSCs, the variance $(\Delta n_0)^2$ is equal to n_0 . The standard deviation in $\Delta m(t)$ around $\bar{m}(t)$ caused by Δn_0 can be derived by substituting $n_0 \pm \Delta n_0$ in Eq. 3 and thus obtaining a $X_3'(t)$. Then

$$\Delta m(t) = x_3'(t) - x_3(t) = \frac{\Delta n_0 k_{23}}{\lambda_1 - \lambda_2} \left\{ \pm e^{-\lambda_1 t} \pm e^{-\lambda_2 t} \right\}$$

where $X_3(t) = \bar{m}(t)$, the average number of channels in the open state at time t , a quantity that can be measured given a sufficiently large number of PSCs. This is seen to be identical to $n_0 (P_{23}(t))^2$. Adding this, as a source of variance, we get

$$\sigma_m^2(t) = m_0 \left\{ e^{-\lambda_2 t} - P_{33}^2(t) \right\}.$$

The variance in the number of open channels for model I is therefore

$$\sigma_m^2(t) = m_0 \left\{ e^{-\lambda_2 t} - \left(\frac{1}{\lambda_1 - \lambda_2} \left((\lambda_1 - k_{21} - k_{23}) e^{-\lambda_2 t} - (\lambda_2 - k_{21} - k_{23}) e^{-\lambda_1 t} \right) \right)^2 \right\}.$$

which we can rewrite as:

$$\sigma_{k_0}^2 = k_0 \left\{ e^{-\lambda_2 t} - \left(\frac{\lambda_1 - B}{\lambda_1 - \lambda_2} \right)^2 e^{-2\lambda_1 t} - \frac{2B(\lambda_1 + \lambda_2 - B) - \lambda_1 \lambda_2}{(\lambda_1 - \lambda_2)^2} e^{-(\lambda_1 + \lambda_2)t} - \left(\frac{\lambda_2 - B}{\lambda_1 - \lambda_2} \right)^2 e^{-2\lambda_2 t} \right\}$$

where $B = k_{21} + k_{23}$. This is a one parameter (B) family of curves. But the range over which B can be varied is found by relating Eq. 3 to Eq. 1.

$$\lambda_2 < k_{21} + k_{23} < (1 - C)\lambda_1 + C\lambda_2.$$

The area that is covered by this family of curves is colored black in Fig. 4. The figure shows that there is a significant gap between the high efficacy curve and the low efficacy family of curves. This gap gets bigger for larger values of C . For our case the gap seems big enough to not allow for any ambiguous experimental data.

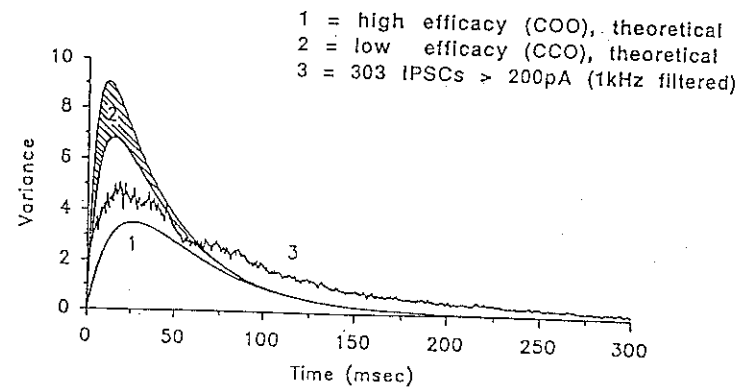


Figure 4 The average of a sample of postsynaptic currents was fitted with $\lambda_1 = 102.4$, $\lambda_2 = 26.3$ and $C = .524$. For both high and low efficacy the theoretical tailvariance with these parameter values is plotted. The experimental tailvariance of the same sample is also plotted.

The actual experimentally observed (see also Fig. 4) variance appears to lie a little bit above the high efficacy curve. This can be explained by assuming a high efficacy model and realizing that there are additional sources of variance:

(i) Open channel noise: an open channel is not conducting at a fixed level, but is rapidly fluctuating within a noiseband of about a fifth of the single channel conductance. Open channel noise is almost completely white on the timescales that we are looking at and that is why we see the experimental variance jump up almost vertically at $t=0$. The total amount of open channel noise is proportional to the number of open channels and we therefore see the experimental variance slowly get closer to the theoretical high efficacy variance during the first 50 msec.

(ii) a third slow exponent: a third very slow λ_3 component in (1) might give a negligible (small A3) contribution to the PSC at $t=0$, but because of its slow decay it can become important in the tail of the tail, when the other exponents have almost completely died out, and that is why after 50 msec in Fig. 4 the measured variance lies above the theoretical curve.

We can thus conclude that there are 2 neurotransmitter-bound open states involved in the decay phase of our PSCs and that the amount of time spent in neurotransmitter bound closed states is negligible. GABA appears to be an efficient neurotransmitter.

References

- [1] Hille, B. 1992. Ionic channels of excitable membranes 2nd edition, Sinauer Associates, Massachusetts.
- [2] Colquhoun, D. and A.G. Hawkes. 1977. Relaxation and fluctuations of membrane currents that flow through drug operated channels. *Proc. R. Soc. Lond. B. Biol. Sci.* 199:231-262.
- [3] Silberberg, S.D. and K.L. Magleby. 1993. Preventing errors when estimating single channel properties from the analysis of current fluctuations. *Biophys. J.* 65: 1570-1584.
- [4] Borst, J.G.G., J.L. Lodder and K.S. Kits. 1994. Large amplitude variability of GABA-ergic IPSCs in melanotropes from *Xenopus laevis*: evidence that quantal size differs between synapses. *J. Neurophysiol.*, 71:639-655.
- [5] Busch, C. and B. Sakmann 1990. Synaptic transmission in hippocampal neurons: numerical reconstruction of quantal IPSCs. In *Cold Spring Harbor Symposia in quantitative biology*, Vol LV, pp. 69-80. Cold Spring Harbor Laboratory, Cold Spring Harbor, New York.
- [6] Borst, J.G.G., K.S. Kits and M. Bier. 1994. Variance analysis of GABA-ergic IPSCs from melanotropes of *Xenopus laevis*. Accepted for publication in *Biophys. J.*